# THERAPEUTIC EFFECTS OF HYPOXIC AND PRO-INFLAMMATORY PRIMING OF MESENCHYMAL STEM CELL-DERIVED EXTRACELLULAR VESICLES IN INFLAMMATORY ARTHRITIS

Alasdair G. Kay[1], Kane Treadwell[2], Paul Roach[3], Rebecca Morgan[2], Rhys Lodge[4], Mairead Hyland[2], Anna M.Piccinini[5], Nicholas Forsyth[6], *Oksana Kehoe[2]

[1]Department of Biology, University of York, York, UK; [2]School of Medicine, Keele University at the RJAH Orthopaedic Hospital, Oswestry, UK; [3]Chemistry Department, Loughborough University, Loughborough, UK; [4]School of Chemistry, University of Nottingham, Nottingham, UK; [5]School of Pharmacy, University of Nottingham, Nottingham, UK; [6]School of Pharmacy and Bioengineering, Keele University, The Guy Hilton Research Laboratories, Hartshill, Stoke on Trent, UK

*Correspondence and requests for materials should be addressed to O.K. (email: o.kehoe@keele.ac.uk)

**Abstract**

Novel biological therapies have revolutionised the management of Rheumatoid Arthritis (RA) but no cure currently exists. Mesenchymal stem cells (MSCs) immunomodulate inflammatory responses through paracrine signalling, including via secretion of extracellular vesicles (EVs) in the cell secretome. We evaluated the therapeutic potential of MSCs-derived small EVs in an antigen-induced model of arthritis (AIA).

EVs isolated from MSCs cultured normoxically (21% $O_2$, 5% $CO_2$), hypoxically (2% $O_2$, 5% $CO_2$) or with a pro-inflammatory cytokine cocktail were applied into the AIA model. Disease pathology was assessed post-arthritis induction through swelling and histopathological analysis of synovial joint structure. Activated CD4+ T cells from healthy mice were cultured with EVs or MSCs to assess deactivation capabilities prior to application of standard EVs *in vivo* to assess T cell polarisation within the immune response to AIA.

All EVs treatments reduced knee-joint swelling whilst only normoxic and pro-inflammatory primed EVs improved histopathological outcomes. In vitro culture with EVs did not achieve T cell deactivation. Polarisation towards CD4+ helper cells expressing IL17a (Th17) was reduced when normoxic and hypoxic EV treatments were applied in vitro. Normoxic EVs applied into the AIA model reduced Th17 polarisation and improved Th17:Treg homeostatic balance.

Priming of MSCs in EV production can be applied to alter the therapeutic efficacy however normoxic EVs present the optimal strategy for broad therapeutic benefit. The varied outcomes observed in MSCs priming may promote EVs optimised for therapies targeted for specific therapeutic priorities. EVs present an effective novel technology with potential for cell-free therapeutic translation.

**Keywords**

Rheumatoid Arthritis, inflammation, immunomodulation, extracellular vesicles, mesenchymal stem cells

## Introduction

Mesenchymal stem cells (MSCs) are a promising therapeutic option owing potential for tissue repair through trilineage differentiation capacity, immunomodulatory properties disrupting T cell proliferation, B cell function and dendritic cell (DCs) maturation; and promoting anti-inflammatory responses mediated through macrophage interactions[1]. Widespread introduction of stem cell therapies has been hindered by inconsistent outcomes at clinical trial and donor variability. Our group has demonstrated the immunomodulatory capacity of both MSCs and their conditioned medium (CM-MSC) to reduce inflammation in a murine antigen-induced arthritis (AIA) model through enhanced Treg function and restored Treg:Th17 ratio[2,3]. MSCs convey their immunomodulatory properties through cell-to-cell contact, autocrine responses and paracrine signalling[1], including through secretion of extracellular vesicles (EVs)[4]. EVs are membrane bound particles that carry a cargo of microRNA (miRNA), mRNA, lipid, carbohydrate and protein signals to facilitate intercellular communication[5-9]. Notably, disease severity in seropositive RA has been linked to EVs signalling[10-15]. MSC-derived EVs have been shown to be beneficial in autoimmune disorders in functioning to modulate autoimmune responses, particularly related to graft rejection and hypertension[16-18] but also in inflammatory arthritis and rheumatic diseases[19-21]. T cells have been shown to recruit EVs released by DCs, suggesting an integral action in orchestrating *in*

64 *vivo* immune responses[22,23]. Furthermore, tolerance in DCs is influenced by CD4+ T cells
65 through EVs-mediated intercellular signalling mediated by transfer of EVs-packaged miRNA[24].

66 We hypothesised that EVs recapitulate the anti-inflammatory and immunomodulatory effects
67 of MSCs in the arthritis model and that priming MSCs during the generation of EVs through
68 hypoxic culture or pro-inflammatory cytokine cocktails will enhance therapeutic outcomes.

69 Identification of the most effective cell source and maintenance conditions for generation of
70 optimally efficacious EVs will accelerate development of EV therapeutics for RA and other
71 regenerative medicine targets. To date, no research has directly examined and contrasted the
72 influence of cell isolation and priming on EVs generation using both hypoxia and pro-
73 inflammatory pre-conditioning of MSCs during production.

74 Here we present novel data utilising priming strategies for MSC-derived EVs applied to the
75 AIA model of inflammatory arthritis. We investigate amelioration of symptoms through
76 reduced swelling and histopathological improvement, and EVs influence on T cell proliferation
77 and polarisation *in vitro* and *in vivo*. We hypothesise that EVs represent a potential
78 therapeutic approach for the treatment of inflammatory arthritis that may encounter less
79 obstacles than cell therapy to widespread application in the clinic.

80

81 **Results**

82 *EVs isolated through differential ultracentrifugation characterise as EVs according to*
83 *internationally agreed criteria*

84 All EVs isolated in this study were enriched using 100,000 x g ultracentrifugation with EV
85 pellets resuspended based on counts of source cells taken at the point of collection, with
86 resuspension of vesicles from 1.0 x $10^6$ MSCs per 30µl.

87 A combination of quantitative and qualitative analyses was performed to confirm isolation of
88 EVs. EV preparations from MSCs cultured under normoxic conditions were assessed by flow
89 cytometry analysis using the MACSPlex exosome kit (Miltenyi Biotec) to identify 37 exosomal
90 surface epitopes, including characteristic exosome markers CD9, CD63 and CD81. EV
91 isolations showed elevated enrichment in mean expression values for CD9 (81.25±5.03%),
92 CD63 (94.59±2.23%) and CD81 (79.41±9.07%) (n=11) (representative example Figure S1A)
93 confirming the identity as EVs. Western blot analysis of MSC lysate and EVs (EV-NormO2)
94 determined positive detection of Alix, a transferrin receptor binding protein involved in
95 multivesicular body (MVB) biogenesis. MVBs are a late endosomal compartment functioning
96 to traffic biomolecules in the form of intralumenal vesicles to either lysosomes for
97 degradation or to the plasma membrane for extracellular secretion[25]. Western blot also
98 confirmed the absence of cytochrome C, an ubiquitous mitochondrial protein acting as
99 negative control (Figure S1B)[26]. Transmission Electron Microscopy (TEM) imaging
100 demonstrated the presence of spherical vesicles in isolated preparations of normoxic and
101 hypoxic EVs in accordance with international standards for single EVs characterisation (Figure
102 S1C). Finally, EVs were characterised for their size distribution and concentration using the
103 Nanopore technology (Izon Science). EV preparations showed a distribution of EV sizes with
104 most prevalent diameter of ~ 200 nm with maximal diameter ~500 nm (Figure S1D-E).
105 Together, these results demonstrate that our differential ultracentrifugation methodology
106 successfully isolates EVs according to internationally agreed criteria. We observed that pro-
107 inflammatory priming of MSCs using the methodology adopted here was possible for a period

108 of 48 hours for collection of CM-MSC, but extended cell culture in the presence of pro-
109 inflammatory cocktail to 72 or 96 hours resulted in consistent reductions in cell numbers
110 below the originally seeded cell numbers, suggestive of induced crisis in the cultured cells
111 (data not shown).

112

113 *Priming of MSCs does not affect total protein content in EV cargo*

114 We set out to determine whether the total protein content in the cargo of EVs was impacted
115 by cell priming. A 4 parameter polynomial nonlinear regression of log-transformed
116 bicinchoninic acid assay (BCA, Pierce Biotechnology) data revealed no significant increase in
117 total protein between conditions EV-2%O2 preparations (81.29±34.82 pg/1.0 x $10^6$ cells; n=8)
118 and EV-Pro-Inflam (69.09±37.38 pg/1.0 x $10^6$ cells; n=9) compared to EV-NormO2
119 (40.43±14.73 pg/1.0 x $10^6$ cells; n=11) ($p>0.05$).

120

121 *Application of MSC-derived EVs ameliorates histopathology and joint swelling in AIA*

122 To assess the therapeutic potential of MSC-derived EVs we introduced each of our primed
123 MSCs EVs treatments into a murine model of inflammatory arthritis and measured effects of
124 treatments on histopathological outcomes. AIA is an acute model of inflammatory arthritis
125 that typically exhibits peak joint swelling at 24 hours post induction with clinical symptoms
126 and histopathological signs that resemble rheumatoid arthritis. We have previously
127 demonstrated the efficacy of MSCs and CM-MSC in ameliorating swelling in AIA[2,3]. In this
128 study, we compared three EV treatments to PBS only vehicle controls, measuring the
129 reduction of joint diameter from peak swelling (day 1). Local administration of EVs into joints
130 significantly reduced joint diameter post-arthritis induction, a quantitative measure

131 proportional to joint swelling. Specifically, EV-NormO2 (day 2 = 4.4±0.6mm, day 3 =
132 8.0±0.6mm, $p<0.01$), EV-2%O2 (day 2 = 7.7±0.8mm, day 3 = 11.0±0.9mm, $p<0.001$) and EV-
133 Pro-Inflam (day 2 = 6.7±1.0mm, day 3 = 11.3±0.9mm, $p<0.001$) all very significantly reduce
134 joint swelling in comparison to PBS vehicle control treatments (day 2 = 0.2±0.8mm, day 3 =
135 2.8±1.0mm) (Figure 1A). Reductions in joint diameter from peak swelling were proportional
136 for all treatment conditions.

137 Histopathological symptoms include immune cell infiltration into the synovium; hyperplasia
138 of the synovial membrane; and extravasation of leukocytes into the synovial joint cavity. We
139 have previously shown that the intra-articular injection of MSC conditioned medium in mice
140 with AIA ameliorates damage as observed through histopathological analysis[3]. Whilst EV-
141 2%O2 overall showed a tendency to reduce total arthritis index (AI) scores (4.92±0.84)
142 compared to PBS controls, this was not statistically significant. For EV-NormO2, this reduced
143 AI score reflected decreases from control scores in hyperplasia of the synovial membrane
144 (1.35±0.22 vs 2.30±0.17) and joint exudate (0.50±0.21 vs 1.68±0.30), whilst EV-Pro-Inflam
145 demonstrated reduced synovial infiltrate (2.0±0.39 vs 3.49±0.24) (Figure 1B). Overall AI
146 showed significant reductions in mice treated with EV-NormO2 (4.20±0.79) and EV-Pro-Inflam
147 (4.08±1.04) compared to PBS control (7.46±0.59) (Figure 1C). Taken together, these results
148 demonstrate EV-NormO2 treatment produced a broad reduction in swelling and
149 improvement in histological outcomes, whilst primed MSCs were effective in reducing
150 swelling, but evidence suggested this was not exclusively through reductions in synovial
151 infiltrate or reduced synovial damage.

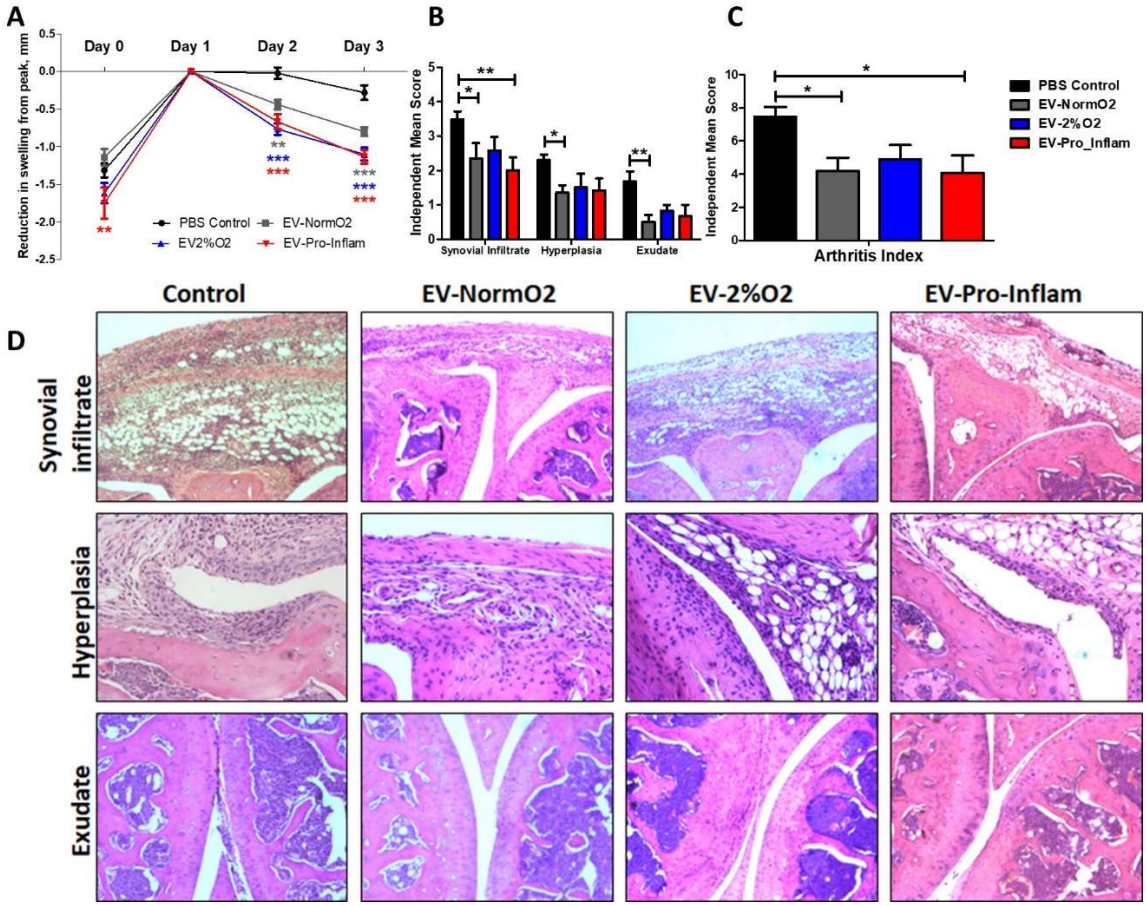


**Figure 1 – MSC-derived EVs treatment of mice with AIA.** (A) Alleviation of joint swelling as a measure of therapeutic efficacy following EV treatments shows a significant effect of EVs compared to vehicle controls at day 2 and day 3 after arthritis induction; normalised to 0 at peak swelling (day 1) (2 Way ANOVA with Repeated Measures and Bonferroni multiple comparisons test post hoc) (B) Examination of histological signs of arthritis pathogenesis following EV treatment shows significant therapeutic effects of EVs sourced from MSCs cultured under normoxia and MSCs cultured in the presence of pro-inflammatory cytokines 3 days post-induction. (C) Combined score arthritis index shows significant reductions in arthritis index 3 days after induction when treated with EVs (1 way ANOVA with Repeated Measures and Bonferroni Multiple Comparisons test post hoc); (D) Representative images for synovial infiltrate, hyperplasia of the synovial lining and synovial exudate into joint cavity for vehicle control and EVs treatments (Control n=21, EV-NormO2 n=8, EV-2%O2 n=6, EV-Pro-Inflam n=6. *p<0.05; **p<0.01; ***p<0.001)

EV-Pro-Inflam treatments showed reductions in synovial infiltrate sufficient to affect a significantly improved overall arthritis index, however this treatment methodology was not as effective at reducing synovial exudate or hyperplasia of the synovial membrane (Figure 1D). The reduction in synovial infiltrate may therefore contribute towards reduced swelling

170 however the results seen in EV-2%O2 suggests this is not a single factor underpinning the
171 mechanism of action.

172

173 *EV treatments do not affect expression of pro- (TNF-α) and anti-inflammatory (IL-10) cytokines*
174 *detectable in serum of AIA mice*

175 The pro-inflammatory cytokine TNF-α is a key driver of disease pathogenesis in RA and a
176 therapeutic target in biological treatments[27,28]. Conversely, IL-10 is a master regulator of anti-
177 inflammatory immune responses[6]. To investigate the effects on circulating cytokines, TNF-α
178 and IL-10 were measured at day 3 in the serum of mice following EV treatments. The
179 circulating concentration of TNF-α in serum of treated mice did not vary significantly between
180 controls (7.02±0.47pg/mL, n=15) and EV treated conditions or between treatments EV-
181 NormO2 (7.38±1.04pg/mL), EV-2%O2 (6.93±0.65pg/mL) or EV-Pro-Inflam (5.73±0.47pg/mL)
182 ($p>0.05$, n=5 per treatment). ELISA on mouse serum could not detect IL-10 in treatment or
183 control conditions (data not shown). Owing to the small volume of synovial fluid in the murine
184 articular cavity, it was not possible to isolate sufficient synovial fluid to accurately detect
185 cytokine expression within the localised joint cavity. The consistent concentrations of
186 circulating TNF-α in serum of mice undergoing treatment and in untreated control mice
187 suggests that immunomodulation of TNF-α regulated cytokine/chemokine induction is not a
188 primary mechanism underpinning efficacy of EVs treatments in reducing swelling and/or
189 histological improvement. This is in contrast to results previously observed in MSC
190 treatments[2].

191

192 *EVs with hypoxic priming or unprimed decrease Th17 polarization but only MSCs suppress*
193 *proliferation when co-cultured with activated CD4+ T cells in vitro*

194 Prior to introduction *in vivo*, we investigated the *in vitro* effect of MSC-derived EVs on T cell
195 polarisation and proliferation to establish an alternative mechanistic rationale for efficacies
196 observed in swelling and histological scores for EVs treatments. MSCs have been shown to
197 deactivate T cells in co-culture[3]. MSCs and EVs produced following conditions EV-NormO2,
198 EV-2%O2 and EV-Pro-Inflam were therefore co-cultured for 5 days with activated T cells
199 isolated from healthy mice and polarisation and proliferation of activated cells assessed as a
200 measure of immune response and T cell deactivation.

201 T cell polarisation was assessed by flow cytometry analysis of surface CD4 and intracellular
202 markers characteristic of Th1 (IFN-γ), Th2 (IL-4) and Th17 (IL-17a). The ability of EV treatments
203 to affect deactivation of T cells, and therefore influence T cell proliferation and extent of
204 immune response, was examined to determine experimental conditions for assessment of EV
205 treatment interactions with T cells *in vivo*.

206 Replicating previous studies[3], MSC with T cell co-cultures prompted significantly increased
207 numbers of CD4+ T cells compared to activated T cells cultured alone. MSCs also elicited
208 increased CD4+ T cells in comparison to EV-2%O2 and EV-Pro-Inflamm treatment conditions
209 ($n=3$, $p<0.05$) but not EV-NormO2 (Figure 2A).

210 Further analysis of IL17a expressing cells within the CD4+ population demonstrated that MSC
211 co-cultures increased cell proportions in comparison to PBS controls and all EV conditions,
212 whereas all EV treatments showed a decrease in Th17 cell polarisation compared to MSCs
213 treatment ($p<0.05$, $n=3$), with both EV-NormO2 and EV-2%O2 treatments showing
214 significantly reduced IL-17a-expressing cells compared to PBS controls ($p<0.001$, $p<0.05$

215 respectively) (Figure 2B). Whilst no differences were seen for IFN-γ expressing cells (Th1)
216 (Figure 2C), IL-4 expressing cells (Th2) were elevated in MSC co-cultures (6.00±0.24%)
217 compared to EV-Pro-Inflam (2.74±0.52%) ($p<0.01$); EV-NormO2 (2.86±0.30%) or EV-2%O2
218 (3.22±0.03%) but not in comparison PBS control (4.79±0.99%) ($p>0.05$, n=3). Notably, EV-
219 NormO2 and EV-Pro-Inflamm treatments reduced proportions of IL4-expressing T cells (Th2)
220 in comparison to PBS controls ($p<0.05$) (Figure 2D). Consequently, pro-inflammatory cocktail
221 priming of MSCs generated EVs that reduced "anti-inflammatory" IL-4-expressing T cells (Th2)
222 but did not reduce IL-17a-expressing, pro-inflammatory T cells (Th17). Statistical analysis was
223 performed using log transformed data.

224 Additionally, the expression of IL17a per cell, represented by mean fluorescence intensity
225 (MFI) of signal, was significantly reduced in EV-NormO2 (3311.74±33.71) and EV-2%O2 T cell
226 co-cultures (3367.19±39.92) compared to CD4+ T cells cultured alone (3728.69±50.28)
227 ($p<0.01$, $p<0.05$, n=3). The impact of this change would need to be assessed *in vivo* as this had
228 not translated to reduced Th17 numbers *in vitro*.

229 These results demonstrate that *in vitro* MSC-derived EVs do not prompt increases in CD4+ T
230 cell numbers or Th17 effector cell polarisation as seen with MSC treatments. Interpretation
231 of this data is limited by the lack of Treg data preventing the examination of the Treg:Th17
232 ratio which is offset in RA.

233

234 We have previously shown the ability of MSCs to suppress T cell proliferation in co-culture,
235 with MSCs being more effective than CM-MSC[3]. MSC with T cell co-culture reduced the
236 proportion of proliferating T cells, measured via a proliferative index[29] and the number of
237 proliferative cycles[30] undergone by T cells in co-culture (5.31±0.38, 4.63±0.17 respectively) in

comparison to T cells cultured alone (6.16±0.10, 5.44±0.25) (n=8, p<0.05). In contrast, CD4+ T cells from healthy (not AIA induced) mice showed no significant inhibition of proliferative cycles when cultured with EV-NormO2 (5.85±0.08, 5.01±0.17), EV-2%O2 (6.01±0.18, 4.97±0.14) or EV-Pro-Inflam (6.28±0.12, 4.95±0.09) (n=8, p>0.05) (Figure 2E).

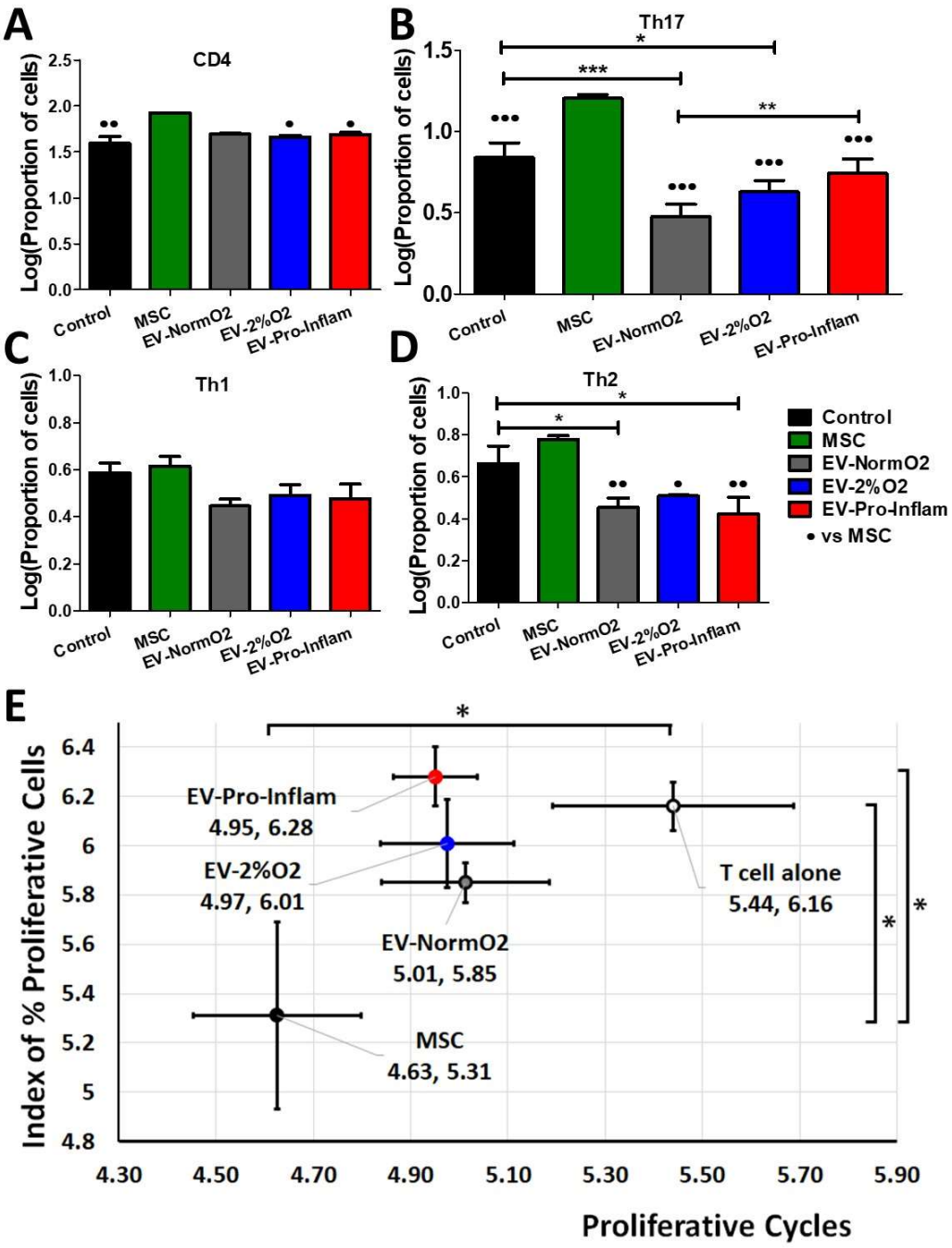


**Figure 2 – Outcomes of EV treatments co-cultured with T cells isolated from healthy murine spleens** **(A)** Increased CD4+ T cells in MSC co-cultures compared to EV-2%O2; EV-Pro-Inflam; and T cells alone

control **(B)** Increased pro-inflammatory Th17 cells (IL17a+) in MSC co-cultures over to EV-NormO2; EV-2%O2; EV-Pro-Inflam; and T cells alone control with EV-NormO2 significantly reduced on PBS control and EV-Pro-Inflamm also **(C)** EV or MSC treatments did not alter Th1 polarisation **(D)** EV treatments all reduced Th2 polarisation in comparison to MSC treatment, with EV-NormO2 and EV-Pro-Inflam also reduced in comparison to PBS controls (Index of proliferation only) (n=3; *p<0.05; **p<0.01; ***p<0.001; 1-Way ANOVA with Bonferroni post-hoc of log transformed data. **(E)** MSC co-cultures significantly inhibited T cell proliferation compared with T cells cultured alone (both measures) and EV-Pro-Inflam co-culture (Index of proliferation only) (n=3; *p<0.05; **p<0.01; ***p<0.001; 1-Way ANOVA with Bonferroni post-hoc of log transformed data.

EV treatments showed greater impact on proliferative cycles than on the proliferative index, though treatments did not significantly vary from either MSC co-cultures or T cells cultured alone, with the exception of pro-inflammatory primed EVs which allowed a higher proliferative index in comparison to MSC co-culture (n=8, p<0.05) (Figure 2E). Previous studies have shown similar results through the application of whole secretome[3]. The results found here suggest that direct deactivation of T cells and immunomodulated T helper polarisation does not provide a primary mechanism for therapeutic action of EVs *in vivo*. Whilst MSCs do display direct immunomodulation of T cells, it may be that MSC-secreted EVs require an intermediate such as DCs to affect similar influence on T cell responses.

*MSC-derived EVs reduce IL-17a-expressing T cell polarisation and restore the Th17:Treg balance ex vivo*

Following on from our *in vitro* study of T cell deactivation using CD4+ T cells of healthy mice, we hypothesised that direct T cell interactions were not likely to be the mechanism through which therapeutic effects are observed following EVs infusion. EV-Pro-Inflam treatments did not influence T cell polarisation however hypoxic priming of MSCs generated EVs capable of influencing Th2 polarisation and Th17 expression (observed through increased mean fluorescence intensity). At this stage, data suggested MSC priming (either 2%O2 or pro-inflammatory cocktail) conveys no beneficial advantage over normoxically produced MSC-EVs

273 in modulating T cell responses or in reducing swelling and affecting improved histological
274 outcomes. Our previous study demonstrated the ability of whole secretome conditioned
275 medium from normoxically grown MSCs to influence T cell polarisation, restoring Treg:Th17
276 homeostasis, and to affect reductions in swelling and tissue damage *in vivo*, similarly not via
277 T cell deactivation when investigated *in vitro*[3]. We apply the AIA model to examine T cell
278 interactions in only EV-NormO2 vesicles comparative to PBS treated controls. Here we aim to
279 elucidate whether EVs affect T helper cells deactivation *in vivo*. Spleens and lymph nodes
280 (inguinal and popliteal) of EV-NormO2 treated AIA mice and PBS controls were dissociated,
281 and CD4+ T cells isolated. These cells represent *in vivo* primed T cells within the inflammatory
282 arthritis environment prior to EVs treatment, isolation and subsequent *in vitro* activation.

283 EV-NormO2 did not increase the proportion of CD4+ T cells in spleen (13.28±0.51%) or lymph
284 nodes (15.04±1.04%) over PBS controls in spleen (14.21±1.07%) or lymph nodes
285 (15.52±1.15%) ($p>0.05$, $n=4$) (Figure S2A, S2B shown with log transformed data).

286 Examination of *in vivo* primed CD4+ T cells activated and cultured *in vitro* for 4 hours in the
287 presence of a membrane transport blocker facilitated evaluation of T cell polarisation. These
288 results demonstrated MSC polarisation of T cells favoured IL-17a expressing T cells (Th17)
289 outcomes as shown previously[3]. RA (and other autoimmune disease) sufferers experience an
290 imbalanced Th17:Treg ratio leading to inappropriate immune responses and tissue damage[31-
291 34] so for the *in vivo* analysis we additionally examined regulatory T cells (Tregs,
292 CD4+CD25+FOXP3+) polarisation to allow calculation of ratios of Th17:Treg to highlight
293 differential changes in polarisation of subsets of helper T cell that could affect the overall
294 homeostatic balance. Percentage data was log transformed for analysis with unpaired T tests
295 (figures show log transformed data).

296 When compared to PBS control (3.23±0.81%), spleen T cell polarisation towards IL17a-
297 expressing T (Th17) effector cells following EV-NormO2 (0.83 ± 0.10%) treatment showed a
298 significant decrease in the proportion of pro-inflammatory Th17 cells induced in AIA mice
299 ($p<0.01$, n=4), with an additional significant decrease in CD4+CD25+FOXP3+ (Treg)
300 proportions in EV-NormO2 treated T cells (0.97 ± 0.05) compared to PBS controls (1.12 ± 0.02)
301 ($p<0.05$, n=4) (Figure 3A). This translated to significantly improved Treg:Th17 ratios in spleens
302 of EV-NormO2 (12.06±2.12:1) treated mice compared to PBS controls (5.03±1.40:1) ($p<0.05$,
303 n=4) (Figure 3B). This result indicates that EVs can prompt an advantageous shift in the
304 Treg:Th17 balance towards a healthy state (EV-NormO2 vs PBS control, 12.06 ± 2.12 vs 5.03
305 ± 1.40, $p<0.05$, n=4), demonstrating a similar efficacy of applying EVs alone to that previously
306 seen when applying CM-MSC[3]. A similar trend was seen in T cells from lymph nodes with a
307 significant reduction in Th17 polarisation in EV (0.90±0.09%) compared with PBS controls
308 (4.26±1.12%) ($p<0.05$, n=4) (Figure 3C) leading to improved Treg:Th17 ratio (EV-NormO2 vs
309 PBS control, 9.01 ± 0.80 vs 3.78 ± 1.80, $p<0.05$, n=4) (Figure 3D). Taken together, these data
310 show that EV treatments were capable of affecting alleviation of symptoms of inflammatory
311 arthritis through reduced Th17 polarisation and shift in the Treg:Th17 balance. We also
312 observed an increase in IFN-γ expressing (pro-inflammatory Th1) T cells in spleens of EV-
313 NormO2 treated mice (6.38±0.40%) compared to PBS controls (4.00±0.35%) ($p<0.05$, n=4)
314 (Figure S2C). Although no change was observed in IL-4 expressing (Th2) T cells (Figure S2D),
315 increased Th1 polarisation lead to an increased Th1:Th2 balance in EV-NormO2 treated mice
316 (3.32 ± 0.27) compared to PBS controls (1.69 ± 0.35) ($p<0.05$, n=4) (Figure S2E). This change
317 was not seen in cells of lymph nodes of these mice (Figure S2F).

318 The outcomes of treatment using EVs *in vivo* demonstrate a reduction in polarisation towards
319 IL17a secreting T helper cells for both spleen and lymph nodes of AIA treated mice that is not

320 seen *in vitro* using EV-treated activated T cells from healthy mice (without AIA induction). We
321 therefore hypothesise that the therapeutic effect seen *in vitro* may require the presence of a
322 mediator and we propose the candidate for this would be DCs. Regulatory T cells influence
323 DCs through EVs mediated intercellular communication to provide immunomodulation,
324 including regulation of tolerance in autoimmune conditions[24]. Potentially the variation
325 observed through *in vivo* treatments compared with *in vitro* responses reflect the absence of
326 mediating cell types such as DCs.

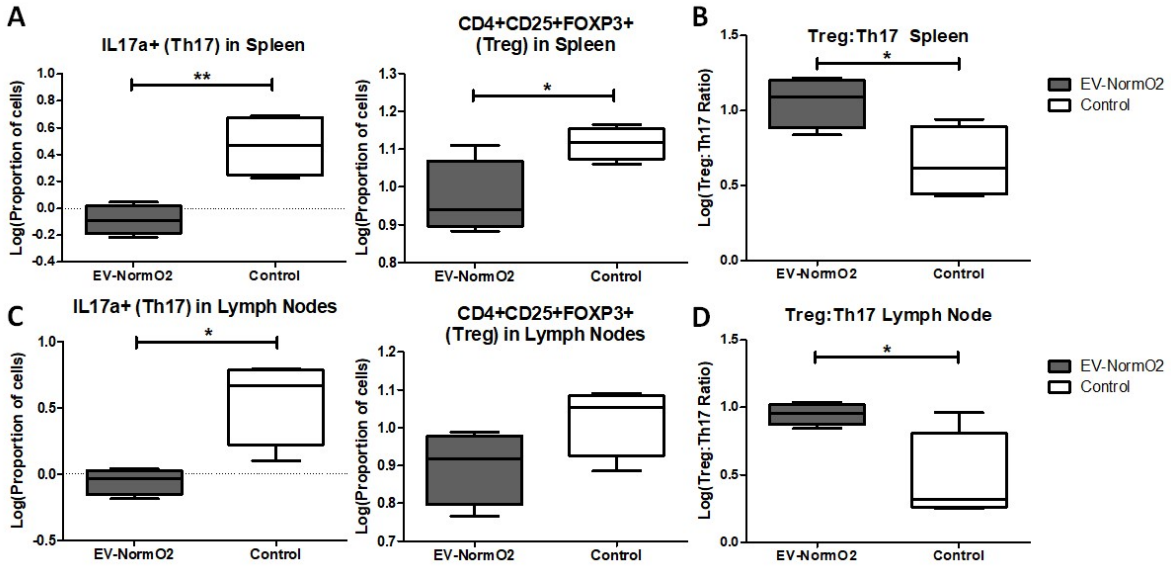


327

328 **Figure 3 – Outcomes of intracellular staining for T cell polarisation analysis. Intracellular staining**
329 **for FACS analysis of IFN-γ, IL4 and IL17a in CD4+ T cells from EV-NormO2 versus PBS control.**
330 **Significant reductions in (A/C) IL17a expression suggestive of reduced Th17 polarisation in Spleen**
331 **and Lymph Node with a small or insignificant change in regulatory T cell polarisation (B/D)**
332 **resulted in trend for restoration of the Treg:Th17 balance in EV-NormO2 treated mice which was**
333 **found significant in lymph node cells only (n=4, *p<0.05; **p<0.01)(Unpaired T Test using log**
334 **transformed data).**

335

336 **Discussion**

337 This study builds on the growing knowledge for the therapeutic efficacy of EVs as a treatment
338 for inflammatory autoimmune disorders. Here, we demonstrated the first application of MSC-

339 derived EVs into the AIA model of inflammatory arthritis with examination of both hypoxic
340 and pro-inflammatory cell priming evaluated against standard EV generation. For this
341 investigation, the AIA model of inflammatory arthritis is pertinent in investigating the T cell
342 mediated inflammatory response, as AIA is specifically driven through CD4+ T-lymphocyte
343 responses leading to synovial leukocyte infiltration[35], in comparison to the more commonly
344 applied collagen-induced arthritis (CIA) model which involves a breach of immune tolerance
345 and generation of systemic polyarticular disease through production of autoantibodies
346 leading to synovitis[36]. Consequently, whilst CIA has recently been applied to evaluate the
347 efficacy of EVs therapies as a model of RA, producing results demonstrating strong
348 immunomodulatory effects with unknown mechanism[19] or indicating T-lymphcyte
349 mechanisms underpin therapeutic outcomes[37], the AIA model remains appropriate for
350 examining molecular changes evoked through the immunomodulatory action of EVs and their
351 impact upon CD4+ T cells[36] as shown in this study. We aim to inform researchers and clinicians
352 on the efficacy of priming strategies to prepare EVs as an enhanced therapy. In our study, EV
353 treatments prompted amelioration of clinical symptoms of AIA with reduction of joint
354 swelling both with and without priming. Examination of joint sections showed improved
355 histological features following standard and pro-inflammatory primed MSC-derived EV
356 treatments compared to controls but not when using hypoxically derived EVs.
357 Mechanistically, EVs acted remarkably different from their cells of origin (MSCs) when co-
358 cultured with CD4+ T cells from healthy murine spleens. Standard and hypoxically-derived EVs
359 reduced Th17 polarization without affecting T cell proliferation, while MSCs increased Th17
360 polarization, and lessened T cell proliferation. Our previous study indicated that MSCs do
361 indeed increase Th17 polarisation but this is offset by increases in Treg cells to restore a more
362 homeostatic balance between the two. Here we examined the Treg:Th17 ratio following AIA

363 initiation and treatment with EV-NormO2. With lack of significant improvements in hypoxic
364 priming outcomes, we opted to test only EV-NormO2 for influence on T cell polarisation
365 following treatment application in the pro-inflammatory environment. *Ex vivo*, CD4+ T cells
366 isolated from spleens of arthritic mice treated with standard EV-NormO2 again showed
367 significantly reduced Th17 polarization that rebalanced the Treg:Th17 ratio. Together, this
368 suggests the reduction in Th17 cells led to restoration of the Treg:Th17 ratio, which is typically
369 unbalanced in inflammatory arthritis, and reduced immune cell recruitment. This result was
370 accompanied with an increase in IFN-γ expressing T cells (Th1) and concomitant increase in
371 the Th1:Th2 ratio which should be taken into account when considering clinical interventions,
372 although for this study the interest was directed towards RA therapies targeting Treg:Th17
373 ratios.

374 To further dissect the therapeutic mechanism of action of MSC-derived EVs, circulating levels
375 of TNF-α, which is a key driver of pathogenesis in RA and therapeutic target in biological
376 treatments, and IL-10, which is a master regulator of anti-inflammatory immune responses,
377 were measured in mice with AIA at day 3. While IL-10 was not detected in our assay, similarly
378 low levels of TNF-α were detected in serum of untreated and EV-treated mice. However,
379 whilst this suggests that TNF-α blockade and IL-10 modulation are not the mechanisms by
380 which MSC-derived EVs improve AIA, it is noted that circulating serum levels of TNF-α rise
381 rapidly in 24 hours post-induction then fall rapidly in the AIA model, so detectable serum TNF-
382 α may not be significantly different in AIA and control mice at 3 days post-induction[38,39]. This
383 mechanism may be more suited to assessment following prophylactic treatment using EVs
384 administered at the point of induction rather than after onset of symptoms.

385 Our previous study demonstrated reductions in Th17 cells following CM-MSC treatment
386 compared to control and MSC treatments. Whilst EVs have been shown to increase Il-10 in
387 macrophages[40], this study indicates that the presence of MSCs, and not just their secretome,
388 may be driving increased IL-10 expression influencing T cell polarisation *in vivo*, and were
389 responsible for the reduction in Th1 and increase in Th2 cells seen in our previous study[3]. In
390 this study we observe an increase in Th1-like cells following EVs treatments. EVs are capable
391 of significantly reducing Th17 cell numbers, however, and this represents a significant finding
392 in the search for immunomodulatory therapeutics for treating autoimmune disorders where
393 an imbalance in T cell polarisation (Treg:Th17) is integral in disease pathology. Moreover, EV
394 treatment in this study resulted in an improved (2.40-fold over controls) Treg:Th17 ratio
395 compared to our previous results using whole CM-MSC treatment (2.13-fold over control) or
396 MSC treatment (1.47-fold over control)[3].

397 The proportions of Treg and Th17 cells in RA sufferers has been directly linked to the severity
398 of disease, and restoring the Treg:Th17 balance has the potential to promote homeostasis
399 and positive clinical outcomes. Here, we demonstrate that untreated (PBS control) spleens of
400 mice with AIA display a Treg:Th17 ratio of 5:1 and that this is improved to 12:1 upon EV-
401 NormO2 treatment. This result reinforces the use of vesicular secretome as a therapeutic
402 option for RA treatment. Furthermore, MSC-EVs have been shown previously to be the
403 component of the secretome responsible for *in vitro* immunosuppression of activated T cell
404 responses[41,42] and our study both replicates and builds on these results through extrapolation
405 to the *in vivo* environment and specific examination of T cells from spleen and lymph nodes
406 isolated from *in vivo* experimentation. We additionally offer data to support the selection of
407 standard culture practices as advantageous in producing broad immunomodulatory

408 outcomes, in comparison to either hypoxic or pro-inflammatory priming of MSCs for EVs
409 production.

410 We observed effects on T cell polarisation that were consistent between *in vitro* and *ex vivo*
411 outcomes, with the exception of reduced Th2 cells *in vitro* being unmatched *ex vivo*.

412 It has been suggested that the immunomodulatory properties of EVs are contingent on pro-
413 inflammatory priming[19,43]. However, the present work demonstrates that whilst priming
414 strategies may enhance some therapeutic outcomes, the mechanisms are unclear and the
415 overall immunomodulatory property may be inherent to MSC-EVs regardless of priming
416 methodology. This would suggest the benefits of priming strategies for EVs production may
417 be dependent on MSC variability. EV-Pro-Inflam were the least effective treatment
418 methodology for T cell deactivation, however they did reduce swelling and immune cell
419 recruitment to the synovium. We hypothesise that these effects are due to alterations in the
420 EV cargo prompted by the culture conditions, with our previous studies demonstrating
421 modulations such as increased chemotaxis and angiogenesis prompted through pro-
422 inflammatory priming of MSCs prior to EVs collection[44]. In contrast, hypoxically primed MSCs
423 produced EVs that reduced swelling but failed to have any impact upon the histological
424 outcomes measured in AIA joints. Neither priming strategy demonstrated consistent
425 improvements in immunomodulatory or tissue regenerative outcomes.

426 Our results suggest that the *in vivo* response to pro-inflammatory primed EV treatment in the
427 AIA model of inflammatory arthritis is not primarily through inhibition of T cell activation, but
428 through suppression of CD4+ Th17 effector polarisation combined with reduction in synovial
429 infiltration in the affected joint. Although this effect is more pronounced following pro-
430 inflammatory priming of MSCs in comparison to standard EV production, the reduction in

431 exudate and hyperplasia seen with EV-NormO2 treatments is likely to convey a greater
432 therapeutic response. Pannus tissue is thought to develop from cells of the synovial
433 membrane and cells infiltrating the joint cavity in response to pro-inflammatory signalling[45,46].
434 The reduction of synovial infiltrate, hyperplasia and synovial exudate observed in EV-NormO2
435 treatments *in vivo* may therefore translate to reduced pannus formation. These benefits, in
436 combination with improved Th17:Treg balance would convey advantageous outcomes in
437 comparison to either priming methodology.

438 We hypothesise that whilst the overall effectiveness of these treatment methodologies is
439 similar in potency, the outcomes differ due to variations in underlying mechanisms of action.
440 Our results demonstrate hypoxic preconditioning reduces swelling *in vivo* and affects Th17
441 polarisation of T cells *in vitro*, however insufficient evidence was found to propose a clear
442 mechanism for therapeutic capacity. MSCs under hypoxic culture have been shown to
443 promote anti-inflammatory M2 macrophage polarization[47], reduce reactive oxygen species
444 (ROS) and upregulate TGF-β, IL-8, IL-10 and PGE2, which are also implicated in macrophage
445 polarisation and MSC immunomodulatory capacity[47-49]. Consequently, we hypothesise that
446 effects seen *in vivo* following hypoxic preconditioning may be related to reduction in
447 macrophage mediated immune responses and more appropriate for tissue regenerative
448 applications. Furthermore, hypoxic culture of MSCs has been shown to promote
449 vascularisation[50,51] which, whilst beneficial for tissue repair, may actually contribute to
450 pannus formation in the RA joint[46]. Given these considerations, the evidence here suggests
451 that normal culture conditions are sufficient to elicit an optimal response in MSCs for EVs
452 production ahead of therapeutic application into the inflammatory environment.

453 Previously, we determined that joint swelling in induced arthritis as a clinical indication of
454 joint inflammation is reduced in the presence of administered MSCs and these cells migrate
455 into the inflamed synovium[2]. Joint swelling is common with different types of arthritis and is
456 caused by oedema due to the endothelial cells of blood vessels becoming leaky in the
457 inflamed synovium. We hypothesised that soluble factors produced by MSCs are responsible
458 for permeability changes in the synovial endothelial cells as these cells did not co-localise,
459 although further studies are required in this regard. The therapeutic potential of MSC-derived
460 EVs has been documented in an animal model of radiation-induced lung injury where EVs
461 attenuated radiation-induced lung vascular damage, inflammation, and fibrosis via miRNA-
462 214-3p[52] and in a rodent model of haemorrhagic shock-induced lung injury model where EVs
463 attenuated pulmonary vascular permeability and lung injury[53].

464 Given the observed outcomes, we hypothesise that the similarities in immunomodulation
465 between EV-2%O2 and EV-Pro-Inflam treatment may lie in their influence on STAT3
466 activation. Increased HIF-1α activates STAT3[54]. STAT3 induces RORγt expression and is
467 activated by TNF-α, IL-6, IL-21 and IL-23, which are key cytokines in promoting Th17
468 differentiation, and RORγt is a master regulator of Th17 differentiation[55,56]. Moreover, STAT3
469 activation has been shown to be necessary for the development of Th17 cells and Th17
470 related autoimmunity, such as seen in RA[56] so EVs inhibiting STAT3 activation could lead to
471 the drop in Th17 polarisation observed. EVs from other mesenchymal cell types are implicated
472 in influencing STAT3 signalling to induce mesenchymal transition[57] and EVs from
473 macrophages are able to trigger nuclear translocation of STAT-3[40], demonstrating STAT3
474 activation as a target of EVs influence. STAT3 has been suggested as a therapeutic target in
475 the treatment of autoimmune inflammatory disorders such as RA[58] and inhibition of STAT3
476 by EVs would have direct therapeutic potential. Furthermore, STAT3 is implicated in

477 interferon responses, which may present a potential mechanism contributing to the increased
478 IFN-γ expressing T cells observed following EV-NormO2 treatments *in vivo*. Further work can
479 elucidate this mechanism of action.

480 In this study, our primary aim was to evaluate the efficacy of EV treatments *in vivo* during AIA.
481 We show that MSC priming leads to the release of EVs that if administered to mice with acute
482 inflammatory arthritis significantly ameliorate disease pathogenesis, mainly through
483 inhibition of Th17 polarization. Future studies will define the composition and sub-vesicular
484 localisation of proteins in EV cargos.

485

486 ***Conclusions***

487 This study provides new evidence that supports the use of EVs in clinical therapies for RA and
488 similar autoimmune disorders. The possibility to manipulate the protein and nucleic acid
489 cargo of EVs through control of parental MSC cultures offers a novel opportunity for targeted
490 therapies that can be tailored to individual pathological features of RA, advancing
491 personalised medicine. Further work on the control of EV cargo will elucidate the molecular
492 mechanism of action underlying varied responses between priming strategies and assist in
493 the efficacy of cell-based therapies in the clinic. This study aims to support the growing body
494 of evidence for the introduction of EVs into the therapeutic milieu.

495

496 **Methods**

497 *Cells and EVs*

498 Primary human MSCs were isolated from commercially available bone marrow aspirate
499 (Lonza, USA) using an adherence technique[48] and each donor material cultured in both
500 normoxic (21%$O_2$) or hypoxic (2%$O_2$) conditions from isolation of MSCs in Dulbecco's
501 Modified Eagles Medium (DMEM) with 10% foetal bovine serum (FBS) and 1% penicillin-
502 streptomycin (n=3 aspirates). Hypoxic cell culture was achieved using 2% $O_2$ in hypoxic
503 workstation (Invivo$_2$ Physiological Cell Culture Workstation, Baker Ruskinn) to ensure cells
504 were not exposed to environmental oxygen levels at any stage of isolation or culture. Cells
505 (P3-P5) were characterised as MSC through immunophenotyping of surface markers with flow
506 cytometry and tri-lineage differentiation[48]. Isolations of EVs were performed over a 48 hour
507 culture period from MSCs in normoxic 21% oxygen culture (EV-NormO2, n=11 isolations);
508 MSCs in hypoxic 2% oxygen culture (EV-2%O2, n=4 isolations) and from MSCs previously
509 cultured for 48 hours with pro-inflammatory cytokine cocktail comprising interferon-gamma
510 (IFN-γ, 10ng/ml), tumour necrosis factor-alpha (TNFα, 10ng/ml) and interleukin 1 beta (IL-1β,
511 5ng/ml) prior to transfer to serum-free medium for 48 hours for EV collection (EV-Pro-Inflam,
512 n=4 isolations).

513

514 *Differential ultracentrifugation for isolation of EVs*

515 MSCs from the same batch used for cell treatment (P3-P5) were cultured to 80-90%
516 confluence in T75 flasks, washed with PBS three times and then serum-free DMEM. Flasks
517 were incubated for 48 hours with 12ml serum-free DMEM at 37°C, 5% $CO_2$. After 48 hours,
518 CM-MSC was removed and a cell count performed to determine the number of cells used to
519 produce EVs. EVs were isolated from CM-MSC by differential ultracentrifugation. In brief, CM-
520 MSC was centrifuged for 10 minutes at 300 *x g* to remove cell debris then again for 10 minutes

521 at 2000 *x g* to remove apoptotic bodies and residual dead cells. Supernatant was again taken
522 and centrifuged at 10,000 *x g* for 45 minutes in an ultracentrifuge (Beckman Coulter) to
523 remove larger/denser EVs. Supernatant was again retrieved and passed through a 0.22µM
524 syringe filter. Filtered supernatant was then centrifuged using fixed angle type 70.1Ti rotor
525 (Beckman Coulter) in a Beckman L8-55M ultracentrifuge, *k*-factor 122.6 at 100,000 *x g* for 90
526 minutes to isolate a pellet comprising small EVs. The EVs pellet was resuspended in 5ml of
527 PBS to wash EVs and then spun again at 100,000 *x g* for 60 minutes, the supernatant discarded
528 and the residual EV pellet resuspended in PBS at 30µL per 1.0 x $10^6$ cells used in EV generation
529 and stored at 4°C to be used within 24 hours or at -20°C for later use.

530

531 *Characterisation of EVs*

532 Successful isolation of EVs was confirmed through multiple methods in accordance with ISEV
533 guidelines[59]. Samples of vesicle preparations underwent BCA for total protein concentration
534 in EV preparations following manufacturer's instructions with EV disruption in a sonicating
535 water bath (30 seconds sonication at 1 minute intervals for 3 cycles) to release intracellular
536 protein and assess cargo proteins as well as surface proteins. Data passed a Kolmogorov-
537 Smirnov test for normality and was analysed with a repeated measures 1 way ANOVA with
538 Tukey's post hoc multiple comparison test.

539 Vesicles were examined using flow cytometry for expression of characteristic markers CD9,
540 CD63 and CD81 (Miltenyi MACSPlex Exosome Identification Kit, human) following
541 manufacturer's instructions for analysis. Particle by particle analysis of vesicle size was
542 assessed using Nanopore technology (Izon Science Ltd) tuned in the region ~80-300nm, to
543 confirm the size fractions being applied experimentally.

544 Images of EVs were obtained using TEM. EVs to be imaged by TEM were isolated as detailed
545 above, however residual EV pellet after PBS wash was resuspended in 30µl Milli-Q water per
546 3.0 x $10^6$ cells. The resulting EV suspension was spotted onto a glow discharged holey carbon
547 mesh copper grids (Quantifoil, R2/1) and incubated at room temperature for 4 mins 45
548 seconds before 5µL of 0.22µm filtered 2% (v/v) uranyl acetate was added. This was left to
549 incubate at room temperature for a further 90 seconds before the excess liquid was removed
550 using blotting paper. Grids were then imaged using a FEI Tecnai G2 12 Biotwin ($LaB_6$,
551 accelerating voltage 100kV).

552 EV protein content was examined by Western Blotting to identify the presence of Alix and
553 absence of mitochondrial Cytochrome C (CYC1) in isolated particles, as per the minimal
554 criteria for identification of EVs[60]. Briefly, ten micrograms of EVs and cells were lysed with 2x
555 Laemlli buffer with β-mercaptoethanol and denatured by heating at 70°C for 5min. Samples
556 were electrophoresed on a 4-12% TGX stain free gel (Bio-Rad, CA, USA) at 200V for 30-40min.
557 Samples were then blotted onto a nitrocellulose membrane using the wet transfer method
558 overnight at 100V. After blotting, membranes were blocked for 2 hours in 5% semi-skimmed
559 milk in Tris-buffered saline with 0.05% Tween (TBST) followed by an incubation in primary
560 antibodies Alix (1:200), CYC1 (1:200) (Santa Cruz Biotechnology, TX, US) for 2 hours at RT.
561 After three five-minute washes, the membrane was probed with a goat anti-mouse IgG-HRP
562 conjugated secondary antibody (1:1,000 in TBST, Life Technologies Limited, Paisley, UK). HRP-
563 conjugated secondary antibody was added for 1h and the wash step repeated. SuperSignal
564 West Femto Chemiluminescent Substrate (Thermo Fisher Scientific, Waltham, MA, USA) was
565 added to the membrane and imaged with ChemiDoc™ Touch Imaging System (Bio-Rad, CA,
566 USA) using Image Lab v.6.0.1 software (Bio-Rad, CA, USA).

567

568 *Co-culture of healthy T cells with EVs*

569 Proliferation of activated T cells was assessed as a measure of T cell deactivation. Initially, for
570 positive controls $5x10^4$ MSCs per well were cultured in 96-well plates for 24 hours at 37°C.
571 CD4+ T cells were purified from spleens and lymph nodes (popliteal/inguinal) of healthy
572 C57Bl/6 mice using the CD4+ T Cell Isolation Kit (Miltenyi) following manufacturer's
573 instructions. T cells were seeded at a density of $5.0x10^5$/well in 250µl RPMI medium with 10%
574 FBS and cultured for 5 days with MSCs (ratio 10:1) or with EV-NormO2, EV-2%O2 or EV-Pro-
575 Inflam (ratio equivalent to secretions from 10:1 cells) (n=8). T cells alone served as control.
576 Cells were activated using anti-Biotin MACSiBead Particles (Miltenyi) (ratio 2:1). EV
577 treatments were refreshed after 2 days of culture. Polarisation was assessed as above and
578 proliferation measured through reduction in signal intensity using VPD450 Violet proliferation
579 dye (BD Biosciences)[3]. Data was analysed using a 2 way repeated measures ANOVA with
580 Bonferroni multiple comparison test post hoc.

581

582 *Antigen-induced arthritis (AIA) model of inflammatory arthritis*

583 Animal procedures were undertaken in accordance with Home Office project licence
584 PPL40/3594. AIA was induced in male C57Bl/6 mice (7-8 weeks) as previously described[2,3,61].
585 Swelling was assessed by measuring the difference in diameter between the arthritic (right)
586 and non-arthritic (left) knee joints (in mm) using a digital micrometer (Kroeplin GmbH) before
587 and at set time points after treatment. Independent experiments were performed to assess
588 swelling and histopathological effects of EV-NormO2 (n=10), EV-2%O2 (n=6) and EV-Pro-
589 Inflam (n=6) compared with PBS controls (n=21) with all EVs sourced from matching MSCs

590 and statistical analysis performed using 2 Way ANOVA for Repeated Measures with
591 Bonferroni Multiple Comparisons Test post hoc; or for *in vivo* primed T cell collections using
592 EV-NormO2 compared with PBS control (n=4) and log transformed data analysed with
593 Unpaired T tests. Peak swelling was observed at 24 hours post-induction and results at
594 subsequent timepoints are expressed in millimetres as reduction from peak swelling.

595

596 *Intra-articular injection of EVs*

597 Treatments comprising 15µl of EVs suspension in PBS corresponding to EV secretions from
598 ~5.0 x $10^5$ cells or PBS alone controls were injected intra-articularly 1 day post arthritis
599 induction with 0.5ml monoject (29G) insulin syringes (BD Micro-Fine, Franklyn Lakes, USA)
600 through the patellar ligament into the right knee joint. Joint diameters were measured at 1,
601 2 and 3 days post injection. Blood, joints, spleen, inguinal and popliteal lymph nodes were
602 collected immediately post-mortem. Four independent experiments were performed to
603 assess primed EVs impact on joint swelling and histopathology (Control n=21, EV-NormO2
604 n=10, EV-2%O2 and EV-Pro-Inflam n=6). A further independent experiment was conducted to
605 address the potential for EV immunomodulation of T cells in the *in vivo* environment in AIA
606 (EV-NormO2 versus PBS controls, n=4 per condition). All measures were taken to reduce
607 animal numbers wherever possible.

608

609 *Arthritis Index*

610 Animals were sacrificed for histological analysis at day 3 post arthritis induction. Joints were
611 fixed in 10% neutral buffered formal saline and decalcified in formic acid for 4 days at 4°C
612 before paraffin embedding. Sections (5µm) were stained with haematoxylin and eosin (H&E)

613 and mounted in Hydromount (National Diagnostics) as described previously[2,3]. H&E sections
614 were scored for hyperplasia of the synovial intima (0=normal to 3=severe), cellular exudate
615 (0=normal to 3=severe) and synovial infiltrate (0=normal to 5=severe) by two independent
616 observers blinded to experimental groups[62]. Scores were summated, producing a mean
617 arthritis index. Data was analysed using a 1 way repeated measures analysis of variance test
618 with Bonferroni multiple comparison test post hoc.

619

620 *Cytokine Quantification.*

621 IL-10 and TNFα in serum and CM-MSC were quantified using mouse Quantikine ELISA IL-10
622 immunoassay (R&D Systems) and TNFα ELISA high sensitivity (eBioscience) respectively,
623 following manufacturer's instructions.

624

625 *T cell polarisation*

626 Spleens and lymph nodes (popliteal/ inguinal) were collected from mice 3 days post-arthritis
627 induction and dissociated as described previously[3]. Splenocytes and pooled lymph node cells
628 were seeded separately at $1.0x10^6$ cells/well in 96-well plates (Sarstedt) in RPMI-1640 with
629 10% FBS, 0.05µg/mL IL-2 and activated with cell stimulation cocktail (eBioscience) for 1 hour
630 prior to adding 10µg/ml brefeldin A (Sigma) and culturing for a further 4 hours. Unstimulated
631 T cells and cells without brefeldin A served as negative controls. Following activation, cells
632 were resuspended in 2mM EDTA in PBS and Tregs (CD4+CD25+FOXP3+) were isolated using
633 the CD4+CD25+ Regulatory T Cell Isolation Kit (Miltenyi) following manufacturer's
634 instructions; or stained for T cell subset identification. For this, cells were permeabilised using
635 permeabilisation buffer kit (eBioscience) and intracellularly stained with anti-mouse IFN-γ

636 (Th1), IL-4 (Th2) or IL17a (Th17) (eBioscience). Cells were analysed on a BD FACS Canto II flow
637 cytometer and comparisons drawn for percentage CD4+ cells and signal intensity (XGeoMean)
638 for each antibody.

639

640 *Statistical analysis*

641 Data were tested for equal variance and normality using D'Agostino & Pearson omnibus
642 normality test. Differences between groups were compared using 1-way ANOVA with
643 Bonferroni post hoc for parametric data or Kruskal-Wallis ANOVA with Dunn's post hoc test
644 for non-parametric, or 2-way ANOVA with Bonferroni correction, as stated. Repeated
645 measures tests using log transformed data was applied to Protein concentration and analysed
646 with log transformed data using a 4 parameter polynomial nonlinear regression to interpolate
647 results from a standard curve. *In vivo* comparisons of EV-NormO2 treatments versus PBS
648 controls were analysed by log transformation of percentage data and comparison using
649 unpaired T tests. All statistical analysis was carried out using Prism 5 (GraphPad software) or
650 IBM SPSS Statistics 24.0, with $P<0.05$ deemed statistically significant. Results are expressed as
651 mean ± standard error of the mean using *$p<0.05$, **$p<0.01$, ***$p<0.001$.

652

653 ***List of abbreviations***

654 *AIA – Antigen Induced Arthritis model*

655 *BCA – Bicinchoninic Acid Protein Assay*

656 *CM-MSC – MSCs derived conditioned medium*

657 *CTSD – Cathepsin D*

658 *CYC1 – Cytochrome C*

659 *DMEM – Dulbecco's Modified Eagle's Medium*

660 *EV-2%O2 – EVs derived from cells cultured in 2% oxygen*

661 *EV-NormO2 – EVs derived from cells cultured in normal environmental oxygen ~21%*

662 *EV-Pro-Inflam – EVs derived from MSCs cultured with pro-inflammatory cytokine stimulation*

663 *EVs – Extracellular vesicles*

664 *FBS – Foetal bovine serum*

665 *FIH – Factor inhibiting Hif-1 protein*

666 *H&E – Haematoxylin and eosin stain*

667 *HIF-1α – Hypoxia inducible factor 1 alpha*

668 *ICAM-1 – Intercellular adhesion molecule 1*

669 *IDO – Indoleamine 2,3-dioxygenase*

670 *IFN-γ – Interferon gamma*

671 *IL-10 – Interleukin 10*

672 *IL-1β – Interleukin 1 beta*

673 *ISEV – International Society of Extracellular Vesicles*

674 *LFA-1 – Leukocyte function associated antigen 1*

675 *MFI – Mean fluorescence intensity*

676 *miRNA – micro ribonucleic acid*

677 *MMPs – Matrix metalloproteins*

678 *MSCs – Mesenchymal stem/stromal cells*

679 *MVBs/MVEs – Multivesicular bodies/endosomes*

680 *NO – Nitric oxide*

681 *PBS – Phosphate buffered saline*

682 *RA – Rheumatoid Arthritis*

683 *RF – Rheumatoid factor*

684 *RISC – RNA-induced silencing complexes*

685 *RORγt – Retinoic acid receptor-related orphan receptor-γt*

686 *ROS – Reactive oxygen species*

687 *TIMPs – Tissue inhibitor of metalloproteinases*

688 *TNF-α – Tissue necrosis factor alpha*

689 *Treg – Regulatory T cell*

690 *VEGF – Vascular endothelial growth factor*

691 *VHL – von Hippel-Lindau ubiquitin ligase*

692 ***Acknowledgements***

693 The authors would like to thank the Nanoscale and Microscale Research Centre, University of

694 Nottingham, for access to TEM facilities. We would like to thank Dr. Mark Platt (Loughborough

695 University, UK) for his assistance in Nanopore technology.

696 ***Declaration of Interest Statement***

697 The authors declare that they have no competing interests

698 ***Funding***

699 This work was supported by the RJAH Orthopaedic Hospital Charity under Grant [G08028];
700 the UK EPSRC/MRC CDT in Regenerative Medicine (Keele University, Loughborough
701 University, the University of Nottingham) under Grant [EP/F500491/1]; Orthopaedic
702 Institute, Ltd under Grant [RPG 171].

703 ***Author's contributions***

704 A.K. performed experimental work, wrote the manuscript and prepared all figures. K.T.
705 provided support and technical skills for T cell investigations. P.R. gave technical expertise
706 on Nanopore technology. R.M. provided support for histological investigations, TEM
707 experiments and discussed and commented on the manuscript. R.L. performed TEM
708 experiments. M.H. performed ELISAs and provided support for *in vivo* work and histological
709 experiments. A.M.P. gave technical advice on data interpretations and presentation and
710 reviewed the manuscript. N.R.F. contributed to experimental design. O.K. conceived and
711 designed the research study, performed *in vivo* experiments, analysed data, wrote and
712 supervised the manuscript. All authors reviewed the manuscript before submission.

713 **References**

714 1 Prockop, D. J. & Oh, J. Y. Mesenchymal stem/stromal cells (MSCs): role as guardians of
715 inflammation. *Mol Ther* **20**, 14-20, doi:10.1038/mt.2011.211 (2012).
716 2 Kehoe, O., Cartwright, A., Askari, A., El Haj, A. J. & Middleton, J. Intra-articular injection of
717 mesenchymal stem cells leads to reduced inflammation and cartilage damage in murine
718 antigen-induced arthritis. *J Transl Med* **12**, 157, doi:10.1186/1479-5876-12-157 (2014).
719 3 Kay, A. G. *et al.* Mesenchymal Stem Cell-Conditioned Medium Reduces Disease Severity and
720 Immune Responses in Inflammatory Arthritis. *Sci Rep* **7**, 18019, doi:10.1038/s41598-017-
721 18144-w (2017).

722 4 Stanton, H. *et al.* ADAMTS5 is the major aggrecanase in mouse cartilage in vivo and in vitro.
723 *Nature* **434**, 648-652 (2005).
724 5 Beer, K. B. *et al.* Extracellular vesicle budding is inhibited by redundant regulators of TAT-5
725 flippase localization and phospholipid asymmetry. *Proc Natl Acad Sci U S A* **115**, E1127-
726 E1136, doi:10.1073/pnas.1714085115 (2018).
727 6 Couper, K. N., Blount, D. G. & Riley, E. M. IL-10: the master regulator of immunity to
728 infection. *J Immunol* **180**, 5771-5777, doi:10.4049/jimmunol.180.9.5771 (2008).
729 7 Kusuma, G. D. *et al.* To Protect and to Preserve: Novel Preservation Strategies for
730 Extracellular Vesicles. *Front Pharmacol* **9**, 1199, doi:10.3389/fphar.2018.01199 (2018).
731 8 Muralidharan-Chari, V., Clancy, J. W., Sedgwick, A. & D'Souza-Schorey, C. Microvesicles:
732 mediators of extracellular communication during cancer progression. *J Cell Sci* **123**, 1603-
733 1611, doi:10.1242/jcs.064386 (2010).
734 9 Raposo, G. & Stoorvogel, W. Extracellular vesicles: exosomes, microvesicles, and friends. *J*
735 *Cell Biol* **200**, 373-383, doi:10.1083/jcb.201211138 (2013).
736 10 Burbano, C. *et al.* Extracellular vesicles are associated with the systemic inflammation of
737 patients with seropositive rheumatoid arthritis. *Sci Rep* **8**, 17917, doi:10.1038/s41598-018-
738 36335-x (2018).
739 11 Arntz, O. J. *et al.* Rheumatoid Arthritis Patients With Circulating Extracellular Vesicles
740 Positive for IgM Rheumatoid Factor Have Higher Disease Activity. *Front Immunol* **9**, 2388,
741 doi:10.3389/fimmu.2018.02388 (2018).
742 12 Messer, L. *et al.* Microparticle-induced release of B-lymphocyte regulators by rheumatoid
743 synoviocytes. *Arthritis Res Ther* **11**, R40, doi:10.1186/ar2648 (2009).
744 13 Lo Cicero, A., Majkowska, I., Nagase, H., Di Liegro, I. & Troeberg, L. Microvesicles shed by
745 oligodendroglioma cells and rheumatoid synovial fibroblasts contain aggrecanase activity.
746 *Matrix Biol* **31**, 229-233, doi:10.1016/j.matbio.2012.02.005 (2012).
747 14 Zhang, H. G. *et al.* A membrane form of TNF-alpha presented by exosomes delays T cell
748 activation-induced cell death. *J Immunol* **176**, 7385-7393,
749 doi:10.4049/jimmunol.176.12.7385 (2006).
750 15 Kim, S. H. *et al.* Exosomes derived from IL-10-treated dendritic cells can suppress
751 inflammation and collagen-induced arthritis. *J Immunol* **174**, 6440-6448,
752 doi:10.4049/jimmunol.174.10.6440 (2005).
753 16 Lee, C. *et al.* Exosomes mediate the cytoprotective action of mesenchymal stromal cells on
754 hypoxia-induced pulmonary hypertension. *Circulation* **126**, 2601-2611,
755 doi:10.1161/CIRCULATIONAHA.112.114173 (2012).
756 17 Mokarizadeh, A. *et al.* Microvesicles derived from mesenchymal stem cells: potent
757 organelles for induction of tolerogenic signaling. *Immunol Lett* **147**, 47-54,
758 doi:10.1016/j.imlet.2012.06.001 (2012).
759 18 Zhang, B. *et al.* Mesenchymal stem cells secrete immunologically active exosomes. *Stem*
760 *Cells Dev* **23**, 1233-1244, doi:10.1089/scd.2013.0479 (2014).
761 19 Cosenza, S. *et al.* Mesenchymal stem cells-derived exosomes are more immunosuppressive
762 than microparticles in inflammatory arthritis. *Theranostics* **8**, 1399-1410,
763 doi:10.7150/thno.21072 (2018).
764 20 Alcaraz, M. J., Compan, A. & Guillen, M. I. Extracellular Vesicles from Mesenchymal Stem
765 Cells as Novel Treatments for Musculoskeletal Diseases. *Cells* **9**, doi:10.3390/cells9010098
766 (2019).
767 21 Ma, D. *et al.* Immunomodulatory effect of human umbilical cord mesenchymal stem cells on
768 T lymphocytes in rheumatoid arthritis. *Int Immunopharmacol* **74**, 105687,
769 doi:10.1016/j.intimp.2019.105687 (2019).
770 22 Thery, C., Ostrowski, M. & Segura, E. Membrane vesicles as conveyors of immune responses.
771 *Nat Rev Immunol* **9**, 581-593, doi:10.1038/nri2567 (2009).

23 Nolte-'t Hoen, E. N., Buschow, S. I., Anderton, S. M., Stoorvogel, W. & Wauben, M. H. Activated T cells recruit exosomes secreted by dendritic cells via LFA-1. *Blood* **113**, 1977-1981, doi:10.1182/blood-2008-08-174094 (2009).
24 Tung, S. L. *et al.* Regulatory T cell-derived extracellular vesicles modify dendritic cell function. *Sci Rep* **8**, 6065, doi:10.1038/s41598-018-24531-8 (2018).
25 Piper, R. C. & Katzmann, D. J. Biogenesis and function of multivesicular bodies. *Annu Rev Cell Dev Biol* **23**, 519-547, doi:10.1146/annurev.cellbio.23.090506.123319 (2007).
26 Akers, J. C., Gonda, D., Kim, R., Carter, B. S. & Chen, C. C. Biogenesis of extracellular vesicles (EV): exosomes, microvesicles, retrovirus-like vesicles, and apoptotic bodies. *J Neurooncol* **113**, 1-11, doi:10.1007/s11060-013-1084-8 (2013).
27 Djouad, F. *et al.* Reversal of the immunosuppressive properties of mesenchymal stem cells by tumor necrosis factor alpha in collagen-induced arthritis. *Arthritis Rheum* **52**, 1595-1603, doi:10.1002/art.21012 (2005).
28 Firestein, G. S. Rheumatoid arthritis in a mouse? *Nat Clin Pract Rheumatol* **5**, 1, doi:10.1038/ncprheum0973 (2009).
29 Angulo, R. & Fulcher, D. A. Measurement of Candida-specific blastogenesis: comparison of carboxyfluorescein succinimidyl ester labelling of T cells, thymidine incorporation, and CD69 expression. *Cytometry* **34**, 143-151 (1998).
30 Que, J., Lian, Q., El Oakley, R. M., Lim, B. & Lim, S.-K. PI3 K/Akt/mTOR-mediated translational control regulates proliferation and differentiation of lineage-restricted RoSH stem cell lines. *Journal of Molecular Signaling* **2**, doi:10.1186/1750-2187-2-9 (2007).
31 Al-Zifzaf, D. S. *et al.* FoxP3+T regulatory cells in Rheumatoid arthritis and the imbalance of the Treg/TH17 cytokine axis. *The Egyptian Rheumatologist* **37**, 7-15, doi:10.1016/j.ejr.2014.06.004 (2015).
32 Arroyo-Villa, I. *et al.* Frequency of Th17 CD4+ T cells in early rheumatoid arthritis: a marker of anti-CCP seropositivity. *PLoS One* **7**, e42189, doi:10.1371/journal.pone.0042189 (2012).
33 Diller, M. L., Kudchadkar, R. R., Delman, K. A., Lawson, D. H. & Ford, M. L. Balancing Inflammation: The Link between Th17 and Regulatory T Cells. *Mediators of Inflammation* **2016**, 1-8, doi:10.1155/2016/6309219 (2016).
34 Noack, M. & Miossec, P. Th17 and regulatory T cell balance in autoimmune and inflammatory diseases. *Autoimmun Rev* **13**, 668-677, doi:10.1016/j.autrev.2013.12.004 (2014).
35 Wong, P. K. *et al.* Interleukin-6 modulates production of T lymphocyte-derived cytokines in antigen-induced arthritis and drives inflammation-induced osteoclastogenesis. *Arthritis Rheum* **54**, 158-168, doi:10.1002/art.21537 (2006).
36 Jones, G. W., Hill, D. G., Sime, K. & Williams, A. S. In Vivo Models for Inflammatory Arthritis. *Methods Mol Biol* **1725**, 101-118, doi:10.1007/978-1-4939-7568-6_9 (2018).
37 Xu, K. *et al.* Human umbilical cord mesenchymal stem cell-derived small extracellular vesicles ameliorate collagen-induced arthritis via immunomodulatory T lymphocytes. *Mol Immunol* **135**, 36-44, doi:10.1016/j.molimm.2021.04.001 (2021).
38 Lewthwaite, J. *et al.* Role of TNF alpha in the induction of antigen induced arthritis in the rabbit and the anti-arthritic effect of species specific TNF alpha neutralising monoclonal antibodies. *Ann Rheum Dis* **54**, 366-374, doi:10.1136/ard.54.5.366 (1995).
39 Kobayashi, H. *et al.* Antigen induced arthritis (AIA) can be transferred by bone marrow transplantation: Evidence that interleukin 6 is essential for induction of AIA. *Journal of Rheumatology* **29**, 1176-1182 (2002).
40 Bellmunt À, M., López-Puerto, L., Lorente, J. & Closa, D. Involvement of extracellular vesicles in the macrophage-tumor cell communication in head and neck squamous cell carcinoma. *PLoS One* **14**, e0224710, doi:10.1371/journal.pone.0224710 (2019).

41 Blazquez, R. *et al.* Immunomodulatory Potential of Human Adipose Mesenchymal Stem Cells Derived Exosomes on in vitro Stimulated T Cells. *Front Immunol* **5**, 556, doi:10.3389/fimmu.2014.00556 (2014).

42 Monguio-Tortajada, M. *et al.* Nanosized UCMSC-derived extracellular vesicles but not conditioned medium exclusively inhibit the inflammatory response of stimulated T cells: implications for nanomedicine. *Theranostics* **7**, 270-284, doi:10.7150/thno.16154 (2017).

43 Maumus, M. *et al.* Utility of a Mouse Model of Osteoarthritis to Demonstrate Cartilage Protection by IFNgamma-Primed Equine Mesenchymal Stem Cells. *Front Immunol* **7**, 392, doi:10.3389/fimmu.2016.00392 (2016).

44 Hyland, M., Mennan, C., Wilson, E., Clayton, A. & Kehoe, O. Pro-Inflammatory Priming of Umbilical Cord Mesenchymal Stromal Cells Alters the Protein Cargo of Their Extracellular Vesicles. *Cells* **9**, doi:10.3390/cells9030726 (2020).

45 Fassbender, H. G. & Simmling-Annefeld, M. The potential aggressiveness of synovial tissue in rheumatoid arthritis. *The Journal of Pathology* **139**, 399-406, doi:https://doi.org/10.1002/path.1711390314 (1983).

46 Shiozawa, S., Shiozawa, K. & Fujita, T. Morphologic observations in the early phase of the cartilage-pannus junction. Light and electron microscopic studies of active cellular pannus. *Arthritis Rheum* **26**, 472-478, doi:10.1002/art.1780260404 (1983).

47 Takizawa, N. *et al.* Bone marrow-derived mesenchymal stem cells propagate immunosuppressive/anti-inflammatory macrophages in cell-to-cell contact-independent and -dependent manners under hypoxic culture. *Exp Cell Res* **358**, 411-420, doi:10.1016/j.yexcr.2017.07.014 (2017).

48 Kay, A. G. *et al.* BMP2 repression and optimized culture conditions promote human bone marrow-derived mesenchymal stem cell isolation. *Regen Med* **10**, 109-125, doi:10.2217/rme.14.67 (2015).

49 Li, B. *et al.* Hypoxia-Induced Mesenchymal Stromal Cells Exhibit an Enhanced Therapeutic Effect on Radiation-Induced Lung Injury in Mice due to an Increased Proliferation Potential and Enhanced Antioxidant Ability. *Cell Physiol Biochem* **44**, 1295-1310, doi:10.1159/000485490 (2017).

50 Bader, A. M. *et al.* Hypoxic Preconditioning Increases Survival and Pro-Angiogenic Capacity of Human Cord Blood Mesenchymal Stromal Cells In Vitro. *PLoS One* **10**, e0138477, doi:10.1371/journal.pone.0138477 (2015).

51 Leroux, L. *et al.* Hypoxia preconditioned mesenchymal stem cells improve vascular and skeletal muscle fiber regeneration after ischemia through a Wnt4-dependent pathway. *Mol Ther* **18**, 1545-1552, doi:10.1038/mt.2010.108 (2010).

52 Lei, X. *et al.* Mesenchymal Stem Cell-Derived Extracellular Vesicles Attenuate Radiation-Induced Lung Injury via miRNA-214-3p. *Antioxid Redox Signal*, doi:10.1089/ars.2019.7965 (2020).

53 Potter, D. R. *et al.* Mesenchymal stem cell-derived extracellular vesicles attenuate pulmonary vascular permeability and lung injury induced by hemorrhagic shock and trauma. *J Trauma Acute Care Surg* **84**, 245-256, doi:10.1097/ta.0000000000001744 (2018).

54 Almiron Bonnin, D. A. *et al.* Secretion-mediated STAT3 activation promotes self-renewal of glioma stem-like cells during hypoxia. *Oncogene* **37**, 1107-1118, doi:10.1038/onc.2017.404 (2018).

55 Zhou, L. *et al.* TGF-beta-induced Foxp3 inhibits T(H)17 cell differentiation by antagonizing RORgammat function. *Nature* **453**, 236-240, doi:10.1038/nature06878 (2008).

56 Harris, T. J. *et al.* Cutting edge: An in vivo requirement for STAT3 signaling in TH17 development and TH17-dependent autoimmunity. *J Immunol* **179**, 4313-4317, doi:10.4049/jimmunol.179.7.4313 (2007).

57 Schweiger, M. W. *et al.* Extracellular Vesicles Induce Mesenchymal Transition and Therapeutic Resistance in Glioblastomas through NF-kappaB/STAT3 Signaling. *Adv Biosyst* **4**, e1900312, doi:10.1002/adbi.201900312 (2020).
58 Gaffen, S. L., Jain, R., Garg, A. V. & Cua, D. J. The IL-23-IL-17 immune axis: from mechanisms to therapeutic testing. *Nat Rev Immunol* **14**, 585-600, doi:10.1038/nri3707 (2014).
59 Thery, C. *et al.* Minimal information for studies of extracellular vesicles 2018 (MISEV2018): a position statement of the International Society for Extracellular Vesicles and update of the MISEV2014 guidelines. *J Extracell Vesicles* **7**, 1535750, doi:10.1080/20013078.2018.1535750 (2018).
60 Lotvall, J. *et al.* Minimal experimental requirements for definition of extracellular vesicles and their functions: a position statement from the International Society for Extracellular Vesicles. *J Extracell Vesicles* **3**, 26913, doi:10.3402/jev.v3.26913 (2014).
61 Glant, T. T. *et al.* Characterization and Localization of Citrullinated Proteoglycan Aggrecan in Human Articular Cartilage. *PLoS One* **11**, e0150784, doi:10.1371/journal.pone.0150784 (2016).
62 Misjak, P. *et al.* The role of citrullination of an immunodominant proteoglycan (PG) aggrecan T cell epitope in BALB/c mice with PG-induced arthritis. *Immunol Lett* **152**, 25-31, doi:10.1016/j.imlet.2013.03.005 (2013).